ACS Chemical Neuroscience

pubs.acs.org/chemneuro Research Article

Aβ42 Double Mutant Inhibits Aβ42-Induced Plasma and Mitochondrial Membrane Disruption in Artificial Membranes, Isolated Organs, and Intact Cells

Ofek Oren, Shani Ben Zichri, Ran Taube, Raz Jelinek, and Niv Papo*

Cite This: ACS Chem. Neurosci. 2020, 11, 1027−1037 Read Online

ACCESS | Metrics & More | Article Recommendations | Supporting Information

ABSTRACT: Destabilization of plasma and inner mitochondrial membranes by extra- and intracellular amyloid β peptide (Aβ42) aggregates may lead to dysregulated calcium flux through the plasma membrane, mitochondrial-mediated apoptosis, and neuronal cell death in patients with Alzheimer's disease. In the current study, experiments performed with artificial membranes, isolated mitochondria, and neuronal cells allowed us to understand the mechanism by which a nonaggregating Aβ42 double mutant (designated $Aβ42_{DM}$) exerts its neuroprotective effects. Specifically, we showed that $Aβ42_{DM}$ protected neuronal cells from Aβ42-induced accumulation of toxic intracellular levels of calcium and from apoptosis. $Aβ42_{DM}$ also inhibited Aβ42-induced mitochondrial membrane potential depolarization in the cells and abolished the Aβ42-mediated decrease in cytochrome *c* oxidase activity in purified mitochondrial particles. These results can be explained in terms of the amelioration by $Aβ42_{DM}$ of Aβ42-mediated changes in membrane fluidity in DOPC and cardiolipin/DOPC phospholipid vesicles, mimicking plasma and mitochondrial membranes, respectively. These observations are also in agreement with the inhibition by $Aβ42_{DM}$ of phospholipid-induced conformational changes in Aβ42 and with the fact that, unlike Aβ42, the Aβ42−$Aβ42_{DM}$ complex could not permeate into cells but instead remained attached to the cell membrane. Although most of the $Aβ42_{DM}$ molecules were localized on the cell membrane, some penetrated into the cytosol in an Aβ42-independent process, and, unlike Aβ42, did not form intracellular inclusion bodies. Overall, we provide a mechanistic explanation for the inhibitory activity of $Aβ42_{DM}$ against Aβ42-induced membrane permeability and cell toxicity and provide confirmatory evidence for its protective function in neuronal cells.

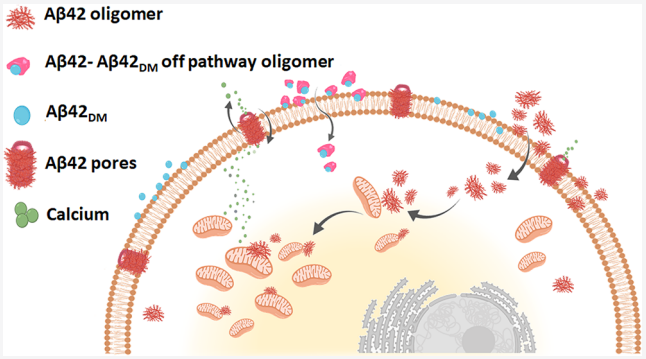

KEYWORDS: *Aβ42 peptide, Alzheimer's disease, amyloids, neurodegeneration, neuronal cell toxicity, protein aggregation, apoptosis, mitochondria, membranes, phospholipids, peptide-lipid interactions*

INTRODUCTION

Aggregation and accumulation of amyloid β (Aβ) peptides in the brains of patients with Alzheimer's disease (AD) is known to be a pathological pathway leading to neurodegeneration.[1,2] The pathological process involves the cleavage by β- and γ-secretase proteolytic enzymes[3] of the transmembrane amyloid precursor protein (APP) (which is also expressed in the brains of healthy people) into Aβ peptides comprising 36−43 residues, the most toxic of which is Aβ42.[4] Aβ42 is released into the extracellular matrix (ECM), where it aggregates into high-order fibrils, leading to the formation of amyloid senile plaques. In addition, emerging evidence has revealed the accumulation of intraneuronal Aβ42 aggregates, which contribute to neuronal toxicity in mouse models of AD and in AD patients.[5,6] These intracellular Aβ42 aggregates are generated in membrane-containing intracellular organelles, such as the endoplasmic reticulum (ER) and the Golgi apparatus,[5−7] by different mechanisms that facilitate the uptake of extracellular Aβ42. These mechanisms include (i) active transport via plasma membrane receptors, such as α7 nicotinic acetylcholine receptors (α7 nAChR), apolipoprotein E (APOE) receptors, members of the low-density lipoprotein receptor (LDLR) family, and other receptors;[8−13] and (ii) intracellular and plasma phospholipid membrane destabilization and permeation pathways.[14,15]

Aβ42 toxicity is far from being fully understood, but it is commonly held that one of the major causes of this neurotoxicity is mediated by the interactions between intra-

Received: November 27, 2019
Accepted: March 10, 2020
Published: March 10, 2020

https://dx.doi.org/10.1021/acschemneuro.9b00638
ACS Chem. Neurosci. 2020, 11, 1027−1037

and/or extracellular Aβ42 peptides, on the one hand, and plasma and intracellular membrane phospholipids, on the other hand.[6,15,16] For the interaction of extracellular Aβ42 with phospholipids, a variety of binding and disruption patterns have been observed,[14,15,17] with the particular pattern depending on the phospholipid composition and the site of measurement (whether inner or outer membrane leaflets/layers). This interaction results in the formation in the plasma membrane of Aβ42 pores, which facilitate an unregulated influx of small molecules and ions, such as Ca^{2+}, into the neuronal cell. Once inside the cell, Aβ42 disrupts the activity of cellular components, such as the ER, mitochondria, endosomes, multivesicular bodies, lysosomes, and the trans-Golgi network.[5−7,18,19] For example, recent studies have shown that Aβ42 is transported into the mitochondria, to the cristae of the inner mitochondrial membrane, via the activity of the translocase of the outer membrane (TOM) machinery, a protein complex found on the outer mitochondrial membrane.[20] Aβ42 has also been shown to interact with apoptotic proteins, such as BIM-BH3,[21] located inside the mitochondria and to cause a reduction in the activity of respiratory enzymes located on the inner mitochondrial membrane, such as cytochrome *c* oxidase (COX). Both the elevated intracellular calcium levels and the mitochondrial damage caused by Aβ42 eventually lead the cells to an apoptotic pathway.[18,19,22−24] The above Aβ42-mediated cytotoxic effects, which are the result of interactions of aggregated Aβ42 with plasma and mitochondrial phospholipid membranes, indicate the urgent need to develop inhibitors of aggregated Aβ42−phospholipid interactions. Studies designed to fulfill this need must therefore address interactions of the aggregated amyloid with plasma and mitochondrial membrane phospholipids, on the one hand, and potential inhibitors, on the other hand.

A necessary first step in such a study would be to design and test artificial phospholipid membrane vesicles that mimic both plasma and mitochondrial membranes, and numerous studies have indeed used artificial membranes with different phospholipid compositions to explore the interactions of Aβ peptides with plasma and intracellular membranes. Recent studies have shown that Aβ42 aggregates can cause the destabilization of vesicles composed of 1,2-dioleoyl-*sn*-glycero-3-phosphocholine (DOPC), a lipid that serves to mimic the plasma membrane phospholipid composition.[25−27] Other studies have employed vesicles mimicking the inner mitochondrial membrane,[21] with some being designed to contain cardiolipin (CL),[21,28,29] a lipid that is found exclusively in the inner mitochondrial membrane[30,31] and has previously been shown to play a significant role in amyloid−membrane interactions.[32] Among the studies testing inhibitors against Aβ42 aggregation and Aβ42-induced neuronal cell toxicity, some have focused on Aβ fragments Aβ(39−42) and others on the plant-based substances, epigallocatechin gallate (EGCG), curcumin, and bacoside-A, all of which have been shown to successfully reduce the Aβ42-mediated disruption/damage to vesicles mimicking the plasma membrane.[33−35] Nevertheless, studies of inhibitors of Aβ interactions with lipid vesicles mimicking both the plasma and the mitochondrial membranes are lacking, as are complementary studies addressing both extracellular and intracellular Aβ toxicity and aggregation in intact cells and intracellular organs. There is therefore a parallel lack of the comprehensive understanding of the inhibition mechanism/s of the different inhibitors that is a prerequisite to developing effective inhibitors of Aβ aggregation.

Our innovative approach to the above problem derives from our previous work showing that an Aβ42 variant, designated A$\beta42_{DM}$, that carries two mutations, F19S and L34P, and exhibits diminished aggregation capabilities[36] can efficiently inhibit both intracellular and extracellular wild-type Aβ42 aggregation and neuronal cell toxicity by modulating the Aβ42 aggregation pathway to produce "off-pathway" oligomers that are nontoxic.[37] In that study, we showed that the plasma membrane internalization, the accumulation, and the toxicity in neuronal cells of these "off-pathway" wild-type Aβ42 oligomers is significantly reduced.[37] In addition, we posited that inhibition by A$\beta42_{DM}$ of Aβ42 plasma membrane internalization results from the ability of the mutant to modulate the interaction of Aβ42 with mitochondrial and plasma membrane phospholipids. In the current study, we show that A$\beta42_{DM}$ does not disrupt artificial plasma and inner mitochondrial phospholipid membranes but rather it inhibits Aβ42-induced fluidity enhancement in those membranes. We also show that, in experiments with intact neuronal cells and isolated inside-out oriented submitochondrial particles (SMPs), A$\beta42_{DM}$ exhibits an inhibitory effect against the Aβ42-mediated enhancement of calcium influx through the plasma membrane, of mitochondrial membrane depolarization, and of COX activity and that it abolishes Aβ42-mediated apoptosis. Taken together, these findings indicate that A$\beta42_{DM}$ may be an exciting new type of lead compound in the treatment of AD.

RESULTS

A$\beta42_{DM}$ Exhibits Lower Cell Internalization Ability than Aβ42 and Remains Mostly Localized on the Membrane. As mentioned above, we have previously demonstrated that the interaction of Aβ42 with A$\beta42_{DM}$ results in the formation of "off-pathway" oligomers, namely, structures that prevent Aβ42 internalization into cells via the plasma membrane, leading to reduced toxicity to neuronal cells.[37] These results led us to posit that the interactions of A$\beta42_{DM}$ with the plasma membrane would differ from those of Aβ42. Indeed, we observed here that while Aβ42 oligomers mostly penetrated into cells of the SH-SY5Y neuroblastoma cell line and formed intracellular aggregates/inclusion bodies (Figures 1A and S1A), A$\beta42_{DM}$ was largely localized on the cell membrane and did not form intracellular inclusion bodies

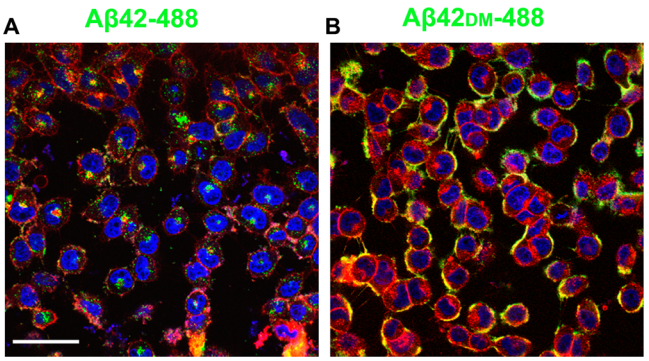

Figure 1. Aβ42 is internalized into SH-SY5Y cells more than A$\beta42_{DM}$. SH-SY5Y cells were incubated with 500 nM Aβ42- (A) or A$\beta42_{DM}$- (B) HiLyte 488-labeled peptides for 18 h. FM-4-64 dye was used to stain the cell membrane; Hoechst stain was used for nuclear staining. Live imaging was performed using an Olympus confocal microscope. Scale bar corresponds to 150 mm.

https://dx.doi.org/10.1021/acschemneuro.9b00638
ACS Chem. Neurosci. 2020, 11, 1027−1037

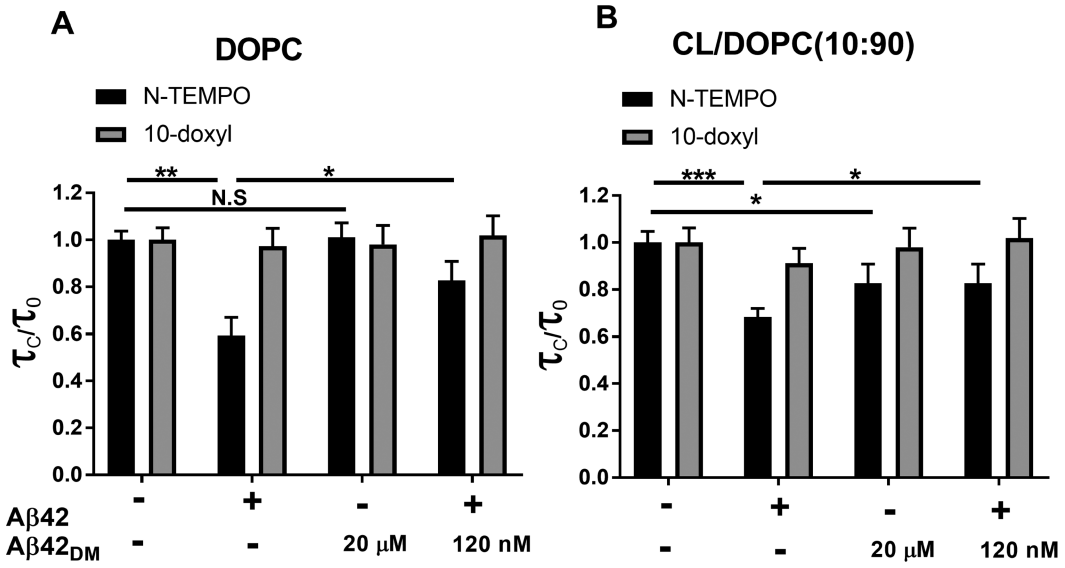

Figure 2. Aβ42$_{DM}$ reduces phospholipid membrane fluidity resulting from Aβ42 interactions with the biomimetic membranes: (A) DOPC, a liposome composition that mimics the plasma membrane, and (B) CL/DOPC (10:90), a liposome composition that mimics the mitochondrial membrane. Changes in the rotation correlation time ratio resulting from peptide−phospholipid interactions were analyzed by ESR spectroscopy. The peptides included in each reaction were Aβ42 (20 μM), Aβ42$_{DM}$ (20 μM), or Aβ42 (20 μM) combined with Aβ42$_{DM}$ (120 nM). The spin probes N-TEMPO and 10-doxyl nonadecane were used to detect changes in fluidity on the membrane surface or in the interior of the membrane, respectively. Statistical analysis (n = 3) was performed with an unpaired Student's t test. *P < 0.05; **P < 0.01; ***P < 0.001. Error bars indicate the standard error of independent experiments performed in triplicate.

(Figures 1B and S1B). Most of the Aβ42$_{DM}$ molecules were localized on the cell membrane, although some penetrated into the cytosol (Figure S2) in an Aβ42-independent process (Figure S3). The Aβ42$_{DM}$ molecules that penetrated the cells were diffused throughout the cytosol, did not accumulate in lysosomes, and, unlike Aβ42, did not form intracellular inclusion bodies (Figure S2).

Since the described phenotype of noninternalization of Aβ42$_{DM}$ is similar to the previously described phenotype of the "off-pathway" and nontoxic Aβ42−Aβ42$_{DM}$ complex, we aimed to further explore whether the differences in the internalization tendencies of Aβ42, Aβ42$_{DM}$, and the Aβ42−Aβ42$_{DM}$ complex also correlated with differences in their interactions with membrane phospholipids (as it has been shown that Aβ42 directly interacts and disrupts membrane phospholipids[14,15]).

Aβ42$_{DM}$ Reduces Aβ42-Mediated Changes in the Fluidity of Artificial Membranes That Mimic the Plasma and Inner Mitochondrial Membranes. Aβ42-induced cell toxicity is known to be related to the ability of Aβ42 to influence plasma membrane fluidity due to its interactions with the membrane phospholipids.[14,15,17] Thus, after showing that Aβ42 aggregates, but not Aβ42$_{DM}$, permeate into the membrane and form intracellular inclusions, we sought to elucidate whether these differences in membrane penetrability are reflected in the phospholipid plasma membrane fluidity upon exposure to the two peptides, Aβ42 and Aβ42$_{DM}$, each alone or a mixture of the two. To this end, we used a biomimetic system, comprising small unilamellar vesicles (SUVs) made of DOPC, which mimics the plasma membrane. To detect changes in vesicle fluidity resulting from the treatment with the peptides, we used electron spin resonance (ESR). To facilitate the use of this technique, two spin probes, *N*-tempoyl palmitamide (N-TEMPO) and 10-doxyl nonadecane, were embedded into the DOPC for detecting changes in the membrane surface and within the interior of the membrane, respectively. These two spin probes are localized in different regions of the phospholipid membrane bilayer: N-TEMPO within the headgroup region[38] and 10-doxyl nonadecane within the hydrophobic core (via covalent linking to the carbon in position 10 of the acyl chain).[39] DOPC−N-TEMPO/10-doxyl nonadecane SUVs were incubated with Aβ42, Aβ42$_{DM}$, or a combination of the two peptides, and rotation correlation times of the spin probes were obtained from ESR spectra. We showed that, upon treatment with Aβ42, phospholipid membrane fluidity on the vesicle surface was enhanced, but the inner-membrane fluidity, detected by the 10-doxyl nonadecane spin probe, did not change relative to the control (Figure 2A). As opposed to Aβ42, Aβ42$_{DM}$ did not affect the phospholipid membrane fluidity. Moreover, upon incubation of the vesicles with a combination of the two peptides, Aβ42$_{DM}$ significantly reduced the Aβ42-induced phospholipid membrane fluidity enhancement on the membrane surface.

Similar to its action on the plasma membrane fluidity, Aβ42 has been shown to interact with and destabilize the mitochondrial membrane.[24,40,41] We thus aimed at exploring whether Aβ42$_{DM}$ has the same protective effect on the mitochondrial membrane as it does for the plasma membrane. To this end, we used a biomimetic system of SUVs consisting of 10% CL and 90% DOPC to mimic the inner mitochondrial membrane.[30,31] Similar to the ESR experiment described above, N-TEMPO or CL/10-doxyl nonadecane were embedded into the CL/DOPC vesicles for the evaluation of changes in vesicle fluidity in the presence of Aβ42, Aβ42$_{DM}$ or combination of the two peptides. Here, too, upon treatment with Aβ42, the fluidity of the surface of the CL/DOPC vesicles (but not the fluidity of the inner part of the vesicles) increased, while Aβ42$_{DM}$ had only a minor effect on the vesicle surface fluidity (Figure 2B). When the vesicles were exposed to a combination of the two peptides, Aβ42$_{DM}$ significantly suppressed the effect of Aβ42 on the vesicle surface fluidity (Figure 2B; and Figure S4 for the ESR measurements).

https://dx.doi.org/10.1021/acschemneuro.9b00638
ACS Chem. Neurosci. 2020, 11, 1027−1037

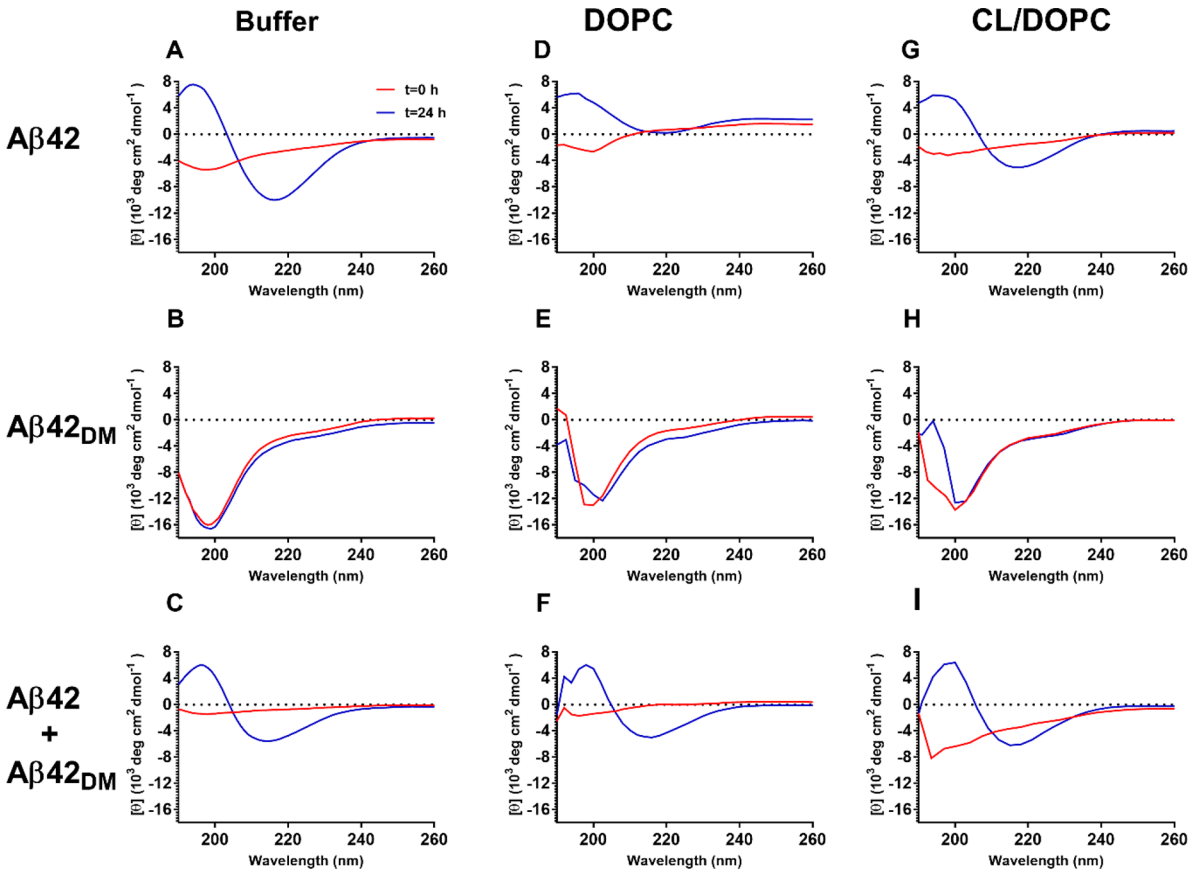

Figure 3. Circular dichroism (CD) spectra of Aβ42 in the absence or presence of Aβ42$_{DM}$ and DOPC or CL/DOPC vesicles. CD spectra of Aβ42 (40 μM), Aβ42$_{DM}$ (40 μM), or a mixture of Aβ42 (40 μM) with Aβ42$_{DM}$ (620 nM) were obtained at a wavelength of 185−260 nm using a quartz cuvette with a path length of 1 mm. Samples were analyzed before incubation (red line) or after 24 h of incubation (blue line) with DOPC or CL/DOPC vesicles in 10 mM sodium phosphate buffer.

In summary, taking together our previous results showing an approximately 50% decrease in the internalization of Aβ42 into cells in the presence of Aβ42$_{DM}$[37] and our current results demonstrating the protective effect of Aβ42$_{DM}$ on Aβ42-mediated disruption of the surface fluidity of the DOPC biomimetic plasma membrane, we conclude that the reduction in the cell penetration ability of Aβ42 in the presence of Aβ42$_{DM}$ is the result of Aβ42$_{DM}$ inhibition of the interaction of Aβ42 with the outer layer of the phospholipid plasma membrane. In addition, our current results showing the protective effect of Aβ42$_{DM}$ against Aβ42-mediated disruption of the fluidity of phospholipid vesicles mimicking the inner mitochondrial membrane suggest that the induction by Aβ42 of the mitochondrial-mediated cytotoxic effect is the result of the interaction of Aβ42 with the CL/DOPC phospholipids and that inhibiting this interaction (as detailed in the following sections) could result in a reduction of Aβ42 toxicity.

Aβ42$_{DM}$ Inhibits Aβ42 Conformational Changes Mediated by DOPC and CL/DOPC Vesicles. As we showed that Aβ42 increased the fluidity of DOPC and CL/DOPC vesicles, while Aβ42$_{DM}$ alone or Aβ42 in the presence of Aβ42$_{DM}$ did not affect vesicle fluidity, we aimed to complement this result by examining first how the structures of Aβ42, Aβ42$_{DM}$, and a combination of Aβ42 and Aβ42$_{DM}$ change upon interaction with DOPC vesicles. Structural changes in the peptides were monitored by circular dichroism (CD) in the presence or absence of DOPC SUVs. Our starting point was previous study showing that in buffer alone Aβ42 (40 μM) is largely unstructured at time zero, but at 24 h it aggregates to exhibit a typical secondary structure with a predominant β-sheet content (Figure 3A and ref 37). However, a significantly different secondary structure, with a much lower β-sheet fraction, was obtained when Aβ42 was incubated for 24 h with DOPC vesicles (Figure 3D). In contrast, Aβ42$_{DM}$(40 μM) did not undergo any structural changes in the presence of vesicles (compared to without vesicles), and a largely random coil secondary structure was maintained (Figure 3B and E). Importantly, a 24 h incubation of Aβ42 (40 μM) with Aβ42$_{DM}$ (620 nM) led to an altered Aβ42 structure, with a reduced β-sheet content, which did not change upon the addition of the vesicles (Figure 3C and F). Similarly, Aβ42 exhibited a different secondary structure, with a lower β-sheet fraction, when aggregated in the presence of CL/DOPC vesicles (mimicking the mitochondrial membrane) as compared to Aβ42 aggregated in the absence vesicles (Figure 3A and G). This result differed from the findings for Aβ42$_{DM}$ or Aβ42 plus Aβ42$_{DM}$, which showed no structural changes in the presence of the vesicles (Figure 3B, H, C, and I). In summary, we found that, in the presence of DOPC or CL/DOPC vesicles, Aβ42 underwent structural changes, while Aβ42$_{DM}$ did not. Moreover, when Aβ42 was incubated with Aβ42$_{DM}$ in the presence of either DOPC or CL/DOPC vesicles, Aβ42 did not undergo structural changes, as opposed to Aβ42 which aggregated in the absence of Aβ42$_{DM}$.

Aβ42$_{DM}$ Reduces the Elevated Intracellular Calcium Levels Mediated by Aβ42. Three lines of investigation

https://dx.doi.org/10.1021/acschemneuro.9b00638
ACS Chem. Neurosci. 2020, 11, 1027−1037

guided this part of the study: (1) studies showing that Aβ42-mediated elevation of intracellular calcium levels in neuronal cells constitutes a key factor in Aβ42-induced cell toxicity, leading to neurodegeneration;[42−44] (2) previous work suggesting that elevated intracellular calcium levels may result from Aβ42 incorporation into the plasma membrane with the consequent perturbation of membrane integrity, eventually leading to a disruption of calcium influx and homeostasis;[44] and (3) our previous observations that Aβ42$_{DM}$ inhibits Aβ42 toxicity in SH-SY5Y cells[37] and that Aβ42$_{DM}$ significantly reduces the plasma membrane destabilization conferred by the interactions of Aβ42 with DOPC. In the current study, we therefore determined intracellular calcium levels in SH-SY5Y cells treated with Aβ42, Aβ42$_{DM}$, or with a combination of Aβ42 and Aβ42$_{DM}$ so as to examine whether the ability of Aβ42$_{DM}$ to prevent Aβ42 from permeating and destabilizing the plasma membrane would lead to inhibition of elevated intracellular calcium levels. We showed that upon exposure of the cells to preformed Aβ42 aggregates (10 μM), intracellular calcium levels were significantly elevated compared to the levels in untreated control cells (Figure 4). However, when the cells were treated with Aβ42 aggregates (10 μM) formed in the presence of Aβ42$_{DM}$ (16 or 64 nM), the Aβ42-mediated intracellular calcium elevation was significantly suppressed (back to background levels) in a dose-dependent manner (Figure 4). Aβ42$_{DM}$ (10 μM) alone also caused a minor increase in the intracellular calcium levels, but to a much smaller extent than that for Aβ42 (Figure 4). These may be explained by the fact that Aβ42$_{DM}$ aggregates at high concentrations, although the structure of these aggregates is different from that of the Aβ42 aggregates. Although Aβ42$_{DM}$ aggregates may be somewhat toxic, their toxicity is expected to be lower than that of Aβ42 due to the different structures of the two peptides.

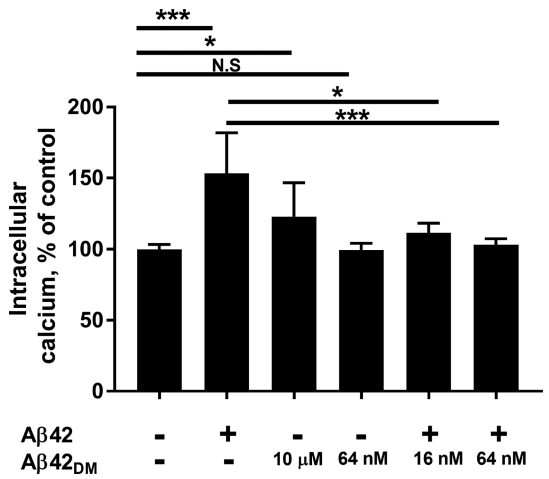

Figure 4. Aβ42$_{DM}$ suppresses the Aβ42-mediated elevation in intracellular calcium levels in SH-SY5Y cells. The cells were incubated with Aβ42$_{DM}$ (10 μM) alone or with preformed Aβ42 aggregates in the presence or absence of Aβ42$_{DM}$ (at molar ratios of 1:625 or 1:156 of Aβ42$_{DM}$/Aβ42) for 48 h, followed by determination of calcium levels using a direct calcium assay (Fluo-4 direct assay kit). Statistical analysis (n = 3) was performed with an unpaired Student's t test. *P < 0.05; **P < 0.01; ***P < 0.001. Error bars indicate the standard error of independent experiments performed in triplicate.

Aβ42$_{DM}$ Suppresses Aβ42-Mediated Mitochondrial Membrane Potential Depolarization. Since increased intracellular calcium levels lead to mitochondrial dysfunction and later to apoptosis,[24] the next stage of the study involved an exploration of the specific effect of Aβ42$_{DM}$ on Aβ42-mediated mitochondrial damage. To this end, we used mitochondrial membrane potential, an established marker for mitochondrial activity,[41] as a measure of Aβ42-mediated mitochondrial damage in the absence and presence of Aβ42$_{DM}$ in SH-SY5Y cells. We showed that, upon exposure of the cells to preformed Aβ42 aggregates, the mitochondrial membrane potential was significantly reduced relative to that in the untreated control cells (Figure 5A). Treatment with Aβ42$_{DM}$ did not affect the mitochondrial membrane potential, and, importantly, for cells exposed to Aβ42 aggregates formed in the presence of Aβ42$_{DM}$, there was a complete suppression of the Aβ42-mediated mitochondrial damage (Figure 5A). This finding is in agreement with our results showing elevated intracellular calcium levels in the presence of Aβ42 and the inhibitory effect of Aβ42$_{DM}$ on intracellular calcium accumulation.

Aβ42-Mediated Damage in Isolated Mitochondrial Particles. The next step was to test whether Aβ42$_{DM}$ can protect against disruption of mitochondrial respiration by Aβ42, as previously shown in isolated mitochondria.[45] To this end, we isolated mitochondria from SH-SY5Y cells and formed inside-out oriented SMPs in which the inner-mitochondrial membrane is exposed to the medium, thereby enabling us to monitor the activity of COX, an established respirometry method to monitor enzyme activity. Since COX plays a crucial role in mitochondrial activity and is known to exhibit reduced activity in AD patients,[46] it can serve as an appropriate measure of the protective effects of Aβ42$_{DM}$ against direct Aβ42 mitochondrial damage. Thus, we evaluated the changes in COX activity in the SMPs in the presence of Aβ42, Aβ42$_{DM}$, or a mixture of Aβ42 and Aβ42$_{DM}$. We showed that, following 24 h of incubation of SMPs with Aβ42, COX activity was significantly reduced, as expected,[45] relative to that for nontreated SMPs (Figure 5B). Aβ42$_{DM}$ alone did not affect COX activity, and, more importantly, when Aβ42$_{DM}$ and Aβ42 were incubated together, the Aβ42-mediated reduction in COX activity was significantly reduced (Figure 5B). These findings indicate that Aβ42$_{DM}$ can protect the mitochondria from direct Aβ42-mediated damage and further highlight the potential of Aβ42$_{DM}$ to serve as a potent Aβ42 inhibitor protecting neuronal cells from Aβ42 toxicity.

Aβ42$_{DM}$ Protects SH-SY5Y Cells from Aβ42-Induced Apoptosis. The final step was to test whether Aβ42$_{DM}$ can protect SH-SY5Y cells from the Aβ42-induced apoptosis previously shown to result from an Aβ42-dependent increase in intracellular calcium levels and mitochondrial damage.[18,19,22−24,42−44] To this end, we followed the rate of apoptosis by FACS with an annexin-V/live/dead kit and showed that upon treatment with preformed Aβ42 aggregates ~34.5% of the cells were apoptotic and 12% were dead, compared to 1.6% apoptotic cells and 3.28% dead cells in control untreated cells (Figure 6). The results for Aβ42$_{DM}$ treatment were 15% apoptotic cells and 1.2% dead cells (Figure 6), values that were significantly lower than those for Aβ42-treated cells. When Aβ42 was allowed to aggregate in the presence of Aβ42$_{DM}$ at different molar ratios (10 μM Aβ42 with 32 or 120 nM Aβ42$_{DM}$), Aβ42$_{DM}$ completely suppressed Aβ42-mediated toxicity in a dose-dependent manner (Figure 6).

https://dx.doi.org/10.1021/acschemneuro.9b00638
ACS Chem. Neurosci. 2020, 11, 1027−1037

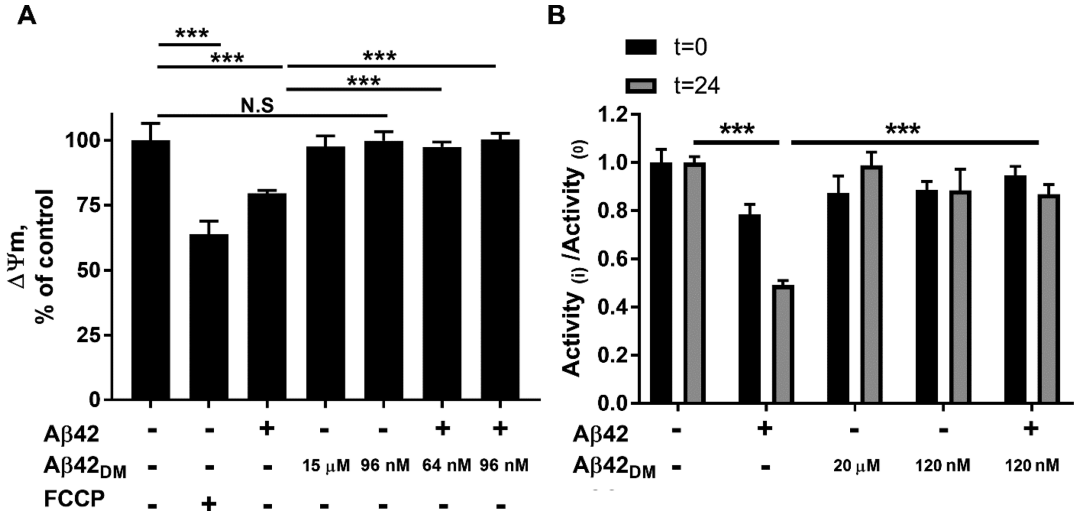

Figure 5. (A) Aβ42$_{DM}$ suppresses the mitochondrial membrane potential depolarization mediated by Aβ42 in SH-SY5Y cells. Cells were incubated with 15 μM Aβ42 aggregates in the presence and absence of Aβ42$_{DM}$ at molar ratio of 1:234 and 1:156 Aβ42$_{DM}$/Aβ42 for 24 h, after which the TMRE mitochondrial membrane potential assay was performed. Carbonyl cyanide-*p*-trifluoromethoxyphenylhydrazone (FCCP) served as the control for depolarization of the mitochondrial membrane potential. The *Y* axis represents the mitochondrial membrane potential ($\Delta\Psi$m). (B) Aβ42$_{DM}$ inhibits damage to COX mediated by Aβ42. SMPs were treated with Aβ42 (20 μM), Aβ42$_{DM}$ (20 μM or 120 nM), or a combination of Aβ42 (20 μM) and Aβ42$_{DM}$ (120 nM). COX absorbance at 550 nm was measured at t = 0 (A) and after 24 h of incubation (B), in the presence of a ferrocytochrome *c* solution (0.22 mM). Statistical analysis (n = 3) was performed with an unpaired Student's t test. *P < 0.05; **P < 0.01; ***P < 0.001. Error bars indicate the standard error of independent experiments performed in triplicate.

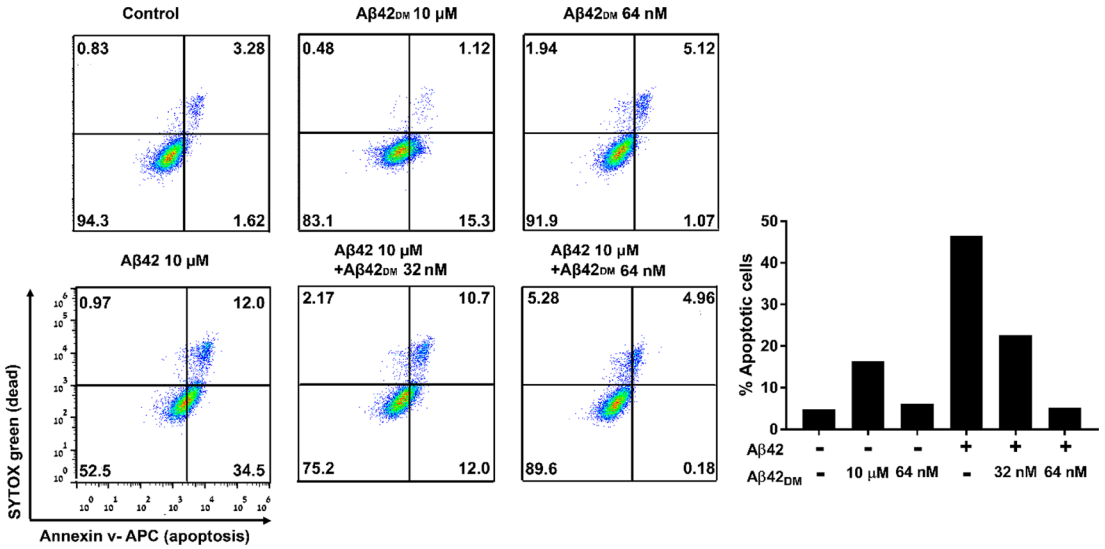

Figure 6. Aβ42$_{DM}$ protects SH-SY5Y cells from Aβ42-induced apoptosis. SH-SY5Y cells were incubated with 10 μM Aβ42 aggregates in the presence or absence of Aβ42$_{DM}$ at molar ratios of 1:312 or 1:625 (Aβ42$_{DM}$/Aβ42) for 48 h. Apoptosis was analyzed by annexin-V staining using FACS. SYTOX Green staining was used to detect dead cells; untreated cells served as a negative control. The values in each quarter (gate) represent the fraction of cells (in percentages) out of the total population.

DISCUSSION

Both the aggregation of Aβ42 and the consequent neuronal cell toxicity have been previously shown to be associated with perturbation of the plasma and mitochondrial membranes, on which Aβ42 peptides self-assemble into peptide−lipid structures.[14−17,20] Numerous mechanisms have been proposed to explain the toxicity of these structures; in particular, it has been posited that they destabilize the membranes, which dysregulates intracellular calcium homeostasis, disrupts the enzymatic activities of mitochondrial respiratory chain complexes III and IV, and induces apoptosis.[40,42−44] To explore these possibilities, we used a nonaggregating,[36] nontoxic Aβ42 double mutant (Aβ42$_{DM}$) that interferes with the formation of the Aβ42 peptide−lipid structures. This double mutant attenuates Aβ42 toxicity,[37] likely because it remains mostly attached to the membrane in a nonaggregated form,[36] as compared with Aβ42 assemblies, which penetrate through the membrane into the cytosol. Notably, a small fraction of Aβ42$_{DM}$ molecules do penetrate into the cytosol; since Aβ42$_{DM}$ is highly active even at low Aβ42$_{DM}$:Aβ42 molar ratios, this small fraction may be sufficient to exert the protective effects of Aβ42$_{DM}$.[37]

Previous studies have shown that the aggregation of Aβ42 promotes a conformation that, unlike the conformation of Aβ42 monomers, and despite the comparable binding affinity

https://dx.doi.org/10.1021/acschemneuro.9b00638
ACS Chem. Neurosci. 2020, 11, 1027−1037

of the two conformations to plasma membranes, facilitates the permeation and destabilization of plasma membrane phospholipids.[25,26] Our results corroborate with these findings and suggest that, whereas Aβ42 increases membrane fluidity,[26] Aβ42$_{DM}$ ameliorates this effect. This finding can explain the ability of Aβ42$_{DM}$ to inhibit the aggregation of Aβ42 and the formation the Aβ42−lipid structures that increase membrane fluidity. It is noteworthy that Aβ42 increased membrane fluidity more in DOPC vesicles than for CL/DOPC vesicles, an unexpected finding because CL is generally known to increase membrane fluidity;[47] a likely explanation is that the inherently high fluidity of the CL/DOPC vesicles has masked the effect of Aβ42. In addition, we found that, in the absence of lipid vesicles, the interaction between Aβ42 and Aβ42$_{DM}$ alters the structure, and, subsequently, the aggregation pattern, of Aβ42 to form nontoxic "off-pathway" oligomers with reduced internalization capabilities.[37] As the structure of Aβ42 does not change when it is coincubated with Aβ42$_{DM}$ in the presence of lipid vesicles, we postulate that the lipids stabilize these "off-pathway" oligomers, and it would be very interesting to elucidate the mechanism underlying this phenomenon through high-resolution (X-ray, NMR) structural analyses. One particularly insightful possibility is a change in the number of solvent-exposed hydrophobic sites, which are key determinants of amyloid toxicity and are important for the interactions with membranes.[48,49]

We also show that Aβ42 reduces COX activity in isolated mitochondria—a finding that is in agreement with a previous study, which showed that stably overexpressing Aβ in SH-SY5Y cells reduces respiration in the mitochondrial complex IV (in which COX is located) but not in complexes I and II.[45] Importantly, however, we also show that Aβ42$_{DM}$ significantly reduces this Aβ42-induced damage. A similar effect was observed in intact cells, where treatment with Aβ42 aggregates increased intracellular calcium levels (indeed, membrane disruption by Aβ42 aggregates is known to dysregulate the influx of calcium ions[50]), while Aβ42$_{DM}$ protected against this damage. Several Aβ42 aggregation inhibitors, such as the mutated recombinant human glucagon-like peptide-1 (mGLP-1) and curcumin, have been previously shown to reduce the Aβ42-induced increase in intracellular calcium.[50,51] Thus, the toxicity of Aβ42 appears to be strongly correlated with its ability to aggregate, an ability that is significantly reduced in the presence of Aβ42$_{DM}$, which does not aggregate at low to medium concentrations. At high concentrations, however, Aβ42$_{DM}$ somewhat increases both the intracellular calcium levels and apoptosis, suggesting that it aggregates to some extent. However, the structure of Aβ42$_{DM}$ aggregates is different and less toxic from those of Aβ42 aggregates and adding Aβ42$_{DM}$ as an inhibitor to Aβ42 does not increase intracellular calcium levels or induces apoptosis. As demonstrated in Oren et al.,[37] Aβ42$_{DM}$ does not reverse Aβ42 aggregation after the formation of the Aβ42 oligomers, indicating that Aβ42$_{DM}$ does not act as a classical competitor. Nevertheless, the inhibitory effect of Aβ42$_{DM}$ does not require that the two peptides are preincubated, suggesting that this inhibition is due to the formation of heteroaggregates, rather than competition.

Considering the findings of this study in light of our previous findings,[37] we believe that the protective mechanism of Aβ42$_{DM}$ derives from its ability to (i) change the extracellular Aβ42 aggregation pathway and reduce its internalization ability, plasma membrane disruption, and downstream intracellular damage; and (ii) penetrate (in small portions) into the cell and reduce the aggregation and toxicity of intracellular Aβ42, including both the Aβ42 peptides that were internalized by reuptake and those produced within the cell.

To conclude, this study provides a mechanistic demonstration, at the levels of artificial membranes, isolated mitochondria, and intact cells, for the mechanism of inhibition of Aβ42 toxicity by Aβ42$_{DM}$. We demonstrate that Aβ42$_{DM}$ binds to Aβ42 aggregates and alters their aggregation pathway into "off-pathway" oligomers. Unlike the well-organized native Aβ42 aggregates and fibrils, these "off-pathway" oligomers exhibit an amorphous structure and, similar to Aβ42$_{DM}$, fewer interactions with membrane phospholipids. Ultimately, Aβ42$_{DM}$ protects the cell against Aβ42-mediated apoptosis by reducing its ability to disrupt the plasma and mitochondrial membranes, penetrate into the cells, and induce mitochondrial damage and intracellular calcium accumulation. Our findings thus highlight the potential of Aβ42$_{DM}$ to serve as an efficient inhibitor of Aβ42-mediated apoptosis and, therefore, as a potential leading compound for the treatment of AD. An *in vivo* study to validate our findings is, therefore, called for.

MATERIALS AND METHODS

Synthetic Peptides. Aβ42 and Aβ42 labeled with HyLight 488 via the N-terminus (Aβ42−488) were purchased from Anaspec (Fremont, CA). Aβ42 bearing the two mutations, F19S and L34P (Aβ42$_{DM}$), was synthesized by and purchased from GL-Biochem (Shanghai, China). Aβ42$_{DM}$-DyLight 488 was generated by free amine labeling of Aβ42$_{DM}$ with DyLight-488 NHS-Ester by using the manufacturer's protocol (Thermo-Fisher, Waltham, MA), and the protein was detected by fluorescent gel (Figure S5A) and Western blot (WB) analysis (Figure S5B) (details describing the WB and fluorescent assays are presented in the Supporting Information). All peptides were dissolved in 10 mM NaOH, aliquoted, and frozen. Peptide concentrations were determined by using a Nanodrop spectrophotometer (extinction coefficient factor 1490 M^{-1} cm^{-1}) (DeNovix, Wilmington, DC). Peptides were allowed to aggregate in 20 mM sodium phosphate buffer, pH 7.4, 0.15 M NaCl at 37 °C with 250 rpm continuous orbital shaking.

Cell Culture. The SH-SY5Y neuroblastoma cell line was a generous gift from Prof. Varda Shoshan-Barmatz (BGU). SH-SY5Y cells were grown at 37 °C and 5% CO_2 in Dulbecco's modified Eagle's medium (DMEM) supplemented with 10% tetracycline-free fetal bovine serum (FBS), L-glutamine (2 mM), and penicillin (100 units/mL)/streptomycin (0.1 mg/mL) (Gibco, Israel).

Confocal Microscopy. SH-SY5Y cells were grown on 1 cm microslides (ibidi, Gräfelfing, Germany). For monitoring Aβ42-488 or Aβ42$_{DM}$-488 localization in cells, SH-SY5Y cells were incubated with 500 nM preformed Aβ42-488 or Aβ42$_{DM}$-488 peptide aggregates. Following 18 h of incubation of the cells with the soluble peptides, images of live cells were taken using an Olympus FV1000 confocal microscope with a long-working distance ×60/1.35 numerical aperture oiled-immersion objective [The National Institute for Biotechnology in the Negev (NIBN), BGU]. Nuclear staining was performed with Hoechst dye (Thermo-Fisher, Israel), diluted 1:200, and membrane staining was performed with FM 4-64 dye at a final concentration of 10 μg/mL (Thermo-Fisher, Waltham, MA).

For lysosomes staining, cells were transfected with 500 ng of Lamp1-GFP gene using Jetoptimus transfection reagent (Polyplus, Illkrich, France) according to the manufacturer's protocol. Later, cells were incubated with 500 nM of Aβ42$_{DM}$ for 18 h, fixed and permeabilized using 4% paraformaldehyde (Thermo-Fisher) and 0.1% Triton (Bio-Lab, Israel), and incubated for 18 h with anti-Aβ42 antibodies (Abcam, Cambridge, MA) diluted 1:200 in PBS followed with incubation anti-Mouse Alexa flour 546 conjugated antibody (Thermo-Fisher) and analyzed in confocal microscopy.

https://dx.doi.org/10.1021/acschemneuro.9b00638
ACS Chem. Neurosci. 2020, 11, 1027−1037

Preparation of Small Unilamellar Vesicles (SUVs). CL (bovine heart) sodium salt, DOPC, N-TEMPO, and 10-doxyl nonadecane were purchased from Avanti Polar Lipids Inc. (Alabaster, AL). Lipid components [DOPC or CL/DOPC (10:90)] were dissolved in a mixture of chloroform/ethanol (1:1) and dried under vacuum to constant weight, followed by addition of phosphate buffer (pH 7.4). For each experiment, vesicles were freshly prepared by probe-sonication of the phospholipid suspension for 10 min at room temperature, with 20% amplitude and on/off 59 s cycles according to a previously published protocol.[52] For all experiments, the final total concentration of lipids was 1 mM, except for the ESR experiment, in which the final lipid concentration was 10 mM.

Electron Spin Resonance. Samples for ESR experiments were prepared using N-TEMPO and 10-doxyl nonadecane as the spin probes. The spin-probes were added to the vesicles (10 mM) in a molar ratio of 500:1 (phospholipid/spin probe), followed by incubation of 20 min at 25 °C. Samples of Aβ42 (20 μM), Aβ42$_{DM}$ (20 μM), or an Aβ42/Aβ42$_{DM}$ (20 μM/120 nM) mixture were mixed with 10 mM DOPC or CL/DOPC (10:90 molar ratio) vesicles, incubated together for 18 h, and placed in glass capillary, 20 mm long and 1 mm ID. ESR spectra were recorded in triplicate using an EPR-mini X-band spectrometer (Spin Ltd., Russia) at room temperature. The modulation 20 G, time constant 0.01, and microwave power level were chosen at subcritical values of 20 mW so as to provide the best signal-to-noise ratio. Rotational correlation time (τ_c) values were calculated from the ESR spectra. Equation 1 was used to determine τ_c:

$$\tau_c = 6.6 \times 10^{-10} \times \Delta H_{(+1)} \left(\sqrt{\frac{I_{(+1)}}{I_{(-1)}}} - 1 \right) \text{(s)} \quad (1)$$

where τ_c is the rotational correlation time; 6.6×10^{-10} is a constant pertinent to the nitroxide spin label; $\Delta H_{(+1)}$ is the low field line width; $I_{(+1)}$ is the low field line height, and $I_{(-1)}$ is the highest field line height.

Circular Dichroism. CD spectra were recorded on a Jasco J715 spectropolarimeter over a range of 185−260 nm using a quartz cuvette with a path length of 1 mm, a scanning speed of 50 nm/min, and a data interval of 0.5 nm, at 25 °C. Aβ42, Aβ42$_{DM}$ (40 μM), or a mixture of Aβ42 (40 μM) with Aβ42$_{DM}$ (620 nM) was analyzed in the absence or presence of DOPC or CL/DOPC (10:90 CL to DOPC molar ratio) vesicles in 10 mM sodium phosphate buffer, pH 7.4, 0.15 M NaCl. Each sample was scanned four times at 0 and 24 h post incubation. Scans were averaged to obtain smooth data and background corrected with respect to protein-free buffer.

Intracellular Calcium Assay. For measuring intracellular calcium levels, 1×10^4 SH-SY5Y cells per well were seeded in black-clear bottomed 96-well plates. Aβ42 (10 μM) peptide was incubated at 37 °C for 18 h in the absence or presence of Aβ42$_{DM}$ at Aβ42$_{DM}$/Aβ42 molar ratios of 1:625 or 1:156. Cells were then treated with the preincubated samples for 48 h. The cells were subjected to an intracellular calcium assay using the Flou-4 Direct Calcium Assay kit (Thermo-Fisher), according to the manufacturer's protocol, which facilitates measurement of the increase in fluorescence relative to a nontreated control as result of increase in the intracellular calcium levels. Changes of fluorescence emission were measured by using a Synergy2 microplate spectrophotometer (BioTek, Winooski, VT) with fluorescence excitation and emission wavelengths of 494 and 516 nm, respectively.

Mitochondrial Membrane Potential Assay. For measuring mitochondrial membrane potential depolarization, 1×10^4 SH-SY5Y cells per well were seeded in black clear-bottomed 96-well plates. Aβ42 (15 μM) peptide was incubated at 37 °C for 18 h in the absence or presence of Aβ42$_{DM}$ at Aβ42$_{DM}$/Aβ42 molar ratios of 1:234 or 1:156. Cells were then treated with the preincubated samples for 24 h. Cells were then analyzed with the TMRE mitochondrial membrane potential assay kit (Abcam, Cambridge, MA) according to the manufacturer's protocol, which facilitates measurement of the reduction in fluorescence relative to untreated control using a Synergy2 microplate spectrophotometer (BioTek) with fluorescence excitation and emission wavelengths of 549 and 575 nm, respectively. FCCP (20 μM) served as the positive control for depolarization of the mitochondrial membrane potential.

Isolation of Mitochondria. For isolation of mitochondria, SH-SY5Y cells were harvested at 75−80% confluence. A mass of 1 g of pelleted cells was rinsed with 10 mL of hypotonic solution (100 mM sucrose, 10 mM MOPS, pH 7.2, 1 mM EGTA) to enable the cells to swell, followed by an incubation of the cells for 10 min on ice according to Panov et al.[53] Thereafter, 2 mL portions of the suspension were homogenized in a Teflon glass homogenizer (Sigma-Aldrich) with gentle circular strokes. The cell suspension was diluted with hypertonic solution (1.25 M sucrose, 10 mM MOPS, pH 7.2) at a ratio of 1 mL of the hypertonic solution to 10 mL of cell suspension so as to restore solution isotonicity. Each cell aliquot was then diluted with six volumes of isolation buffer (75 mM mannitol, 225 mM sucrose, 10 mM MOPS, pH 7.2, 1 mM EGTA, 0.1% fatty acid free BSA). Cellular detritus was precipitated at 2000 rpm for 5 min at 4 °C. The supernatant containing the mitochondria was further centrifuged at 14,000 rpm for 25 min at 4 °C. The crude mitochondrial pellet was rinsed by centrifugation using the same conditions (14,000 rpm, 4 °C for 25 min) in 15 mL of MiR06 buffer (110 mM sucrose, 60 mM K-lactobionate, 20 mM HEPES, pH 7.2, 1 mM KH_2PO_4, 3 mM $MgCl_2 \cdot 6H_2O$, 0.5 mM EGTA, 20 mM taurine, 0.1% fatty acid free BSA).[54] The final pellet was resuspended in 100 μL of MiR06 by vortexing and stored at −80 °C until use.

Preparation of Submitochondrial Particles. A detailed protocol for the preparation of SMPs is described elsewhere.[55] In brief, isolated mitochondria extracted from 1 g of pelleted SH-SY5Y cells was diluted to 2 mL in sonication buffer (250 mM sucrose, 10 mM Tris HCl, 1 mM EDTA, pH 7.0). To form inside-out oriented SMPs (in which the inner mitochondrial membrane faces out to the solution), the suspension of mitochondria was probe sonicated for 30 s at 4 °C using 20% amplitude and 6 s on/off sonication cycles. The molar concentration of SMPs was determined by using a NanoSight NS300 instrument (Malvern Panalytical), with 1 mM DOPC vesicles being used as the calibration standard. The inversion of the inner mitochondrial membrane in SMPs (in such a way that COX is exposed to the environment) was verified by the COX assay described below (Figure S6).

Cytochrome *c* Oxidase Assay. Cytochrome *c* (equine heart), DL-dithiothreitol (DTT), and sodium phosphate monobasic monohydrate and dibasic heptahydrate were obtained from Sigma-Aldrich (Milwaukee, WI). COX activity was determined by monitoring the decrease in absorbance at 550 nm of a chemically reduced ferrocytochrome c solution in the presence of SMPs. Ferrocytochrome *c* substrate solution (0.22 mM) was prepared by addition of 0.1 M DTT to 2.7 mg/1 mL of cytochrome *c* dissolved in purified water. We performed series of measurements of COX activity in the presence of gradually increasing doses of SH-SY5Y SMPs. Figure S4 shows the correlation between SMP concentrations and elevated values of COX activity, which confirms the inversion of the inner mitochondrial membrane within the SMPs. COX is located on the SMP membrane and is exposed to the medium and is therefore available to oxidize the ferrocytochrome *c* substrate. Measurements performed in the presence of Triton-X served as a negative control due to the complete destabilization of membrane and COX inactivation. Samples of SH-SY5Y SMPs (0.1 mM final concentration) were mixed with Aβ42 (20 μM), Aβ42$_{DM}$ (20 μM) or a mixture of Aβ42/Aβ42$_{DM}$ (20 μM/120 nM), and each sample was supplemented with 950 μL of assay buffer (10 mM Tris HCl, 120 mM KCl, pH 7.0). Enzyme buffer (10 mM Tris HCl, 250 mM sucrose pH 7.0) was then added to make the total reaction volume up to 1.1 mL. Finally, 50 μL of ferrocytochrome *c* substrate were added to each mixture, and COX activity was determined (in triplicate) in 200 μL samples in 96-well plates at time 0 and after incubation for 24 h at 37 °C. The kinetic changes of absorbance were measured for 10 min, at 20 s intervals at 25 °C on a BioTek Synergy 4 microplate reader (Winooski, VT). The activity of COX (units/mL) was calculated according to eq 2:

https://dx.doi.org/10.1021/acschemneuro.9b00638
ACS Chem. Neurosci. 2020, 11, 1027−1037

$$\text{COX activity}\left(\frac{\text{units}}{\text{mL}}\right) = \frac{\Delta A \times s^{-1} \times \text{dil} \times V(t)}{V(s) \times 21.84} \quad (2)$$

where $\Delta A\ s^{-1}$ is the reaction rate of a sample subtracted from the blank, 1 unit = 1.0 μmole of ferrocytochrome *c* oxidized per second at pH 7.0, 25 °C; dil is the dilution factor of the ferrocytochrome *c* solution; $V(t)$ is the total reaction volume; $V(s)$ is the volume of ferrocytochrome *c* substrate added to initiate oxidation; and 21.84 is the difference in the extinction coefficients of ferrocytochrome *c* and ferricytochrome *c* at 550 nm.[56]

Detection of Apoptosis by Using Flow Cytometry. For measuring the concentration of apoptotic cells, 1×10^5 SH-SY5Y cells per well were seeded in 24-well plates. A concentration of 10 μM Aβ42 in the absence or presence of 32 or 64 nM Aβ42$_{DM}$ was incubated for 18 h. Cells were then treated with the preincubated samples for 48 h. Thereafter, the cells were harvested, resuspended in phosphate-buffered saline (PBS), and analyzed by using a Beckman Gallios FACS instrument (Indianapolis, IN) for annexin-V-allophycocyanin (APC) and SYTOX Green staining using an annexin-V-APC/dead cells apoptosis kit (Invitrogen, Carlsbad, CA) according to the manufacturer's protocol. Untreated SH-SY5Y cells served as the negative control.

Statistical Analysis. Statistical analysis (n = 3) for the above assays was performed with the unpaired Student's t test, $^*P < 0.05$; $^{**}P < 0.01$; $^{***}P < 0.001$. Error bars indicate the standard error of independent experiments performed in triplicate.

■ ASSOCIATED CONTENT

Supporting Information

The Supporting Information is available free of charge at https://pubs.acs.org/doi/10.1021/acschemneuro.9b00638.

Experimental methods of cytochrome *c* oxidase assay and Western blot analysis, confocal microscopy images of Aβ42−488 and Aβ42$_{DM}$-488, confocal microscopy images of Aβ42$_{DM}$ and lysosomes staining, ESR original spectra, Western blot analysis of Aβ42$_{DM}$ and Aβ42$_{DM}$-488, and cytochrome *c* oxidase activity in SMPs (PDF)

■ AUTHOR INFORMATION

Corresponding Author

Niv Papo − *Avram and Stella Goldstein-Goren Department of Biotechnology Engineering and the National Institute of Biotechnology in the Negev, Ben-Gurion University of the Negev, Beer Sheva 84105, Israel;* orcid.org/0000-0002-7056-2418; Phone: +972-50-2029729; Email: papo@bgu.ac.il

Authors

Ofek Oren − *The Shraga Segal Department of Microbiology, Immunology and Genetics, Faculty of Health Sciences, Ben-Gurion University of the Negev, Beer Sheva 84105, Israel*

Shani Ben Zichri − *Department of Chemistry, Ben-Gurion University, Beer Sheva 84105, Israel*

Ran Taube − *The Shraga Segal Department of Microbiology, Immunology and Genetics, Faculty of Health Sciences, Ben-Gurion University of the Negev, Beer Sheva 84105, Israel*

Raz Jelinek − *Department of Chemistry, Ben-Gurion University, Beer Sheva 84105, Israel;* orcid.org/0000-0002-0336-1384

Complete contact information is available at: https://pubs.acs.org/10.1021/acschemneuro.9b00638

Author Contributions

O.O., S.B.Z., R.J., and N.P. designed the research; O.O. and S.B. performed the research; O.O., S.B.Z., R.T., R.J., and N.P. analyzed the data; O.O. and N.P. wrote the paper. All authors edited the manuscript and approved the final version.

Notes

The authors declare no competing financial interest.

■ ACKNOWLEDGMENTS

The authors thank Dr. Alon Zilka and Dr. Sofiya Kulosheva for their technical assistance. This work was supported by the European Research Council "Ideas program" ERC-2013-StG (Contract Grant Number: 336041) and the Israel Science Foundation (Grant Number 615/14) to N.P.

■ ABBREVIATIONS USED

Aβ, amyloid β; AD, Alzheimer's disease; APP, amyloid precursor protein; Aβ42, amyloid β 1−42; Aβ42$_{DM}$, amyloid β 1−42 double mutant; BGU, Ben-Gurion University of the Negev; BSA, bovine serum albumin; CD, circular dichroism; CL, cardiolipin; COX, cytochrome *c* oxidase; DMEM, Dulbecco's modified Eagle's medium; DOPC, 1,2-dioleoyl-*sn*-glycero-3-phosphocholine; ECM, extracellular matrix; ESR, electron spin resonance; ER, endoplasmic reticulum; FACS, fluorescence activated cell sorting; FBS, fetal bovine serum; FCCP, carbonyl cyanide-*p*-trifluoromethoxyphenylhydrazone; N-TEMPO, *N*-tempoyl palmitamide; PBS, phosphate-buffered saline; SMPs, submitochondrial particles; SUVs, small unilamellar vesicles; WB, Western blot

■ REFERENCES

(1) Nussbaum, J. M., Seward, M. E., and Bloom, G. S. (2013) Alzheimer disease: a tale of two prions. *Prion 7*, 14−19.

(2) Haass, C., and Selkoe, D. J. (2007) Soluble protein oligomers in neurodegeneration: Lessons from the Alzheimer's amyloid β-peptide. *Nat. Rev. Mol. Cell Biol. 8*, 101−112.

(3) Selkoe, D. J. (2003) Folding proteins in fatal ways. *Nature 426*, 900−904.

(4) Bitan, G., Kirkitadze, M. D., Lomakin, A., Vollers, S. S., Benedek, G. B., and Teplow, D. B. (2003) Amyloid β-protein (Aβ) assembly: Aβ40 and Aβ42 oligomerize through distinct pathways. *Proc. Natl. Acad. Sci. U. S. A. 100*, 330−335.

(5) Lee, S. J. C., Nam, E., Lee, H. J., Savelieff, M. G., and Lim, M. H. (2017) Towards an understanding of amyloid-β oligomers: characterization, toxicity mechanisms, and inhibitors. *Chem. Soc. Rev. 46*, 310−323.

(6) LaFerla, F. M., Green, K. N., and Oddo, S. (2007) Intracellular amyloid-β in Alzheimer's disease. *Nat. Rev. Neurosci. 8*, 499−510.

(7) Wilson, C. A., Doms, R. W., and Lee, V. M-Y (1999) Intracellular APP processing and AB production in Alzheimer disease. *J. Neuropathol. Exp. Neurol. 58*, 787−794.

(8) Nagele, R. G., D'Andrea, M. R., Anderson, W. J., and Wang, H.-Y. (2002) Intracellular accumulation of Beta-Amyloid(1−42) in neurons is facilitated by the alpha 7 nicotinic acetylcholine receptor in Alzheimer's disease. *Neuroscience 110*, 199−211.

(9) Snyder, E. M, Nong, Y., Almeida, C. G, Paul, S., Moran, T., Choi, E. Y., Nairn, A. C, Salter, M. W, Lombroso, P. J, Gouras, G. K, and Greengard, P. (2005) Regulation of NMDA receptor trafficking by amyloid-β. *Nat. Neurosci. 8*, 1051−1058.

(10) Zerbinatti, C. V., Wahrle, S. E., Kim, H., Cam, J. A., Bales, K., Paul, S. M., Holtzman, D. M., and Bu, G. (2006) Apolipoprotein E and low density lipoprotein receptor-related protein facilitate intraneuronal Aβ42 accumulation in amyloid model mice. *J. Biol. Chem. 281*, 36180−36186.

(11) Pietrzik, C. U., and Jaeger, S. (2008) Functional role of lipoprotein receptors in Alzheimer's disease. *Curr. Alzheimer Res. 5*, 15−25.

(12) Yazawa, H., et al. (2001) Beta amyloid peptide (Abeta42) is internalized via the G-protein-coupled receptor FPRL1 and forms fibrillar aggregates in macrophages. *FASEB J. 15*, 2454−2462.

(13) Yan, S. D., Chen, X., Fu, J., Chen, M., Zhu, H., Roher, A., Slattery, T., Zhao, L., Nagashima, M., Morser, J., et al. (1996) RAGE and amyloid-β peptide neurotoxicity in Alzheimer's disease. *Nature 382*, 685−691.
(14) Bharadwaj, P., Solomon, T., Malajczuk, C. J., Mancera, R. L., Howard, M., Arrigan, D. W., Newsholme, P., and Martins, R. N. (2018) Role of the cell membrane interface in modulating production and uptake of Alzheimer's beta amyloid protein. *Biochim. Biophys. Acta, Biomembr. 1860*, 1639−1651.
(15) Williams, T. L., and Serpell, L. C. (2011) Membrane and surface interactions of Alzheimer's Aβ peptide-insights into the mechanism of cytotoxicity. *FEBS J. 278*, 3905−3917.
(16) Rauk, A. (2008) Why is the amyloid beta peptide of Alzheimer's disease neurotoxic? *Dalton Trans. 10*, 1273−1282.
(17) Bode, D. C., Freeley, M., Nield, J., Palma, M., and Viles, J. H. (2019) Amyloid-β oligomers have a profound detergent-like effect on lipid membrane bilayers, imaged by atomic force and electron microscopy. *J. Biol. Chem. 294*, 7566−7572.
(18) Umeda, T., Tomiyama, T., Sakama, N., Tanaka, S., Lambert, M. P., Klein, W. L., and Mori, H. (2011) Intraneuronal amyloid β oligomers cause cell death via endoplasmic reticulum stress, endosomal/lysosomal leakage, and mitochondrial dysfunction in vivo. *J. Neurosci. Res. 89*, 1031−1042.
(19) Cho, D. H., Nakamura, T., Fang, J., Cieplak, P., Godzik, A., Gu, Z., and Lipton, S. A. (2009) β-Amyloid-related mitochondrial fission and neuronal injury. *Science 324*, 102−105.
(20) Hansson Petersen, C. A., Alikhani, N., Behbahani, H., Wiehager, B., Pavlov, P. F., Alafuzoff, I., Leinonen, V., Ito, A., Winblad, B., Glaser, E., and Ankarcrona, M. (2008) The amyloid β-peptide is imported into mitochondria via the TOM import machinery and localized to mitochondrial cristae. *Proc. Natl. Acad. Sci. U. S. A. 105*, 13145−13150.
(21) Malishev, R., Nandi, S., Smilowicz, D., Bakavayev, S., Engel, S., Bujanover, N., Gazit, R., Metzler-Nolte, N., and Jelinek, R. (2019) Interactions between BIM protein and beta-amyloid may reveal a crucial missing link between Alzheimer's disease and neuronal cell death. *ACS Chem. Neurosci. 10*, 3555−3564.
(22) Resende, R., Ferreiro, E., Pereira, C., and Resende de Oliveira, C. (2008) Neurotoxic effect of oligomeric and fibrillar species of amyloid-beta peptide 1−42: Involvement of endoplasmic reticulum calcium release in oligomer-induced cell death. *Neuroscience 155*, 725−737.
(23) Keil, U., Bonert, A., Marques, C. A., Scherping, I., Weyermann, J., Strosznajder, J. B., Müller-Spahn, F., Haass, C., Czech, C., Pradier, L., Müller, W. E., and Eckert, A. (2004) Amyloid β-induced changes in nitric oxide production and mitochondrial activity lead to apoptosis. *J. Biol. Chem. 279*, 50310−50320.
(24) Bhat, A. H., Dar, K. B., Anees, S., Zargar, M. A., Masood, A., Sofi, M. A., and Ganie, S. A. (2015) Oxidative stress, mitochondrial dysfunction and neurodegenerative diseases; a mechanistic insight. *Biomed. Pharmacother. 74*, 101−110.
(25) Vestergaard, M. d., Hamada, T., and Takagi, M. (2008) Using model membranes for the study of amyloid beta: lipid interactions and neurotoxicity. *Biotechnol. Bioeng. 99*, 753−763.
(26) Morita, M., Vestergaard, M. D., Hamada, T., and Takagi, M. (2010) Real-time observation of model membrane dynamics induced by Alzheimer's amyloid beta. *Biophys. Chem. 147*, 81−86.
(27) Van Meer, G., Voelker, D. R., and Feigenson, G. W. (2008) Membrane lipids: where they are and how they behave. *Nat. Rev. Mol. Cell Biol. 9*, 112−124.
(28) Gobbi, M., Re, F., Canovi, M., Beeg, M., Gregori, M., Sesana, S., Sonnino, S., Brogioli, D., Musicanti, C., Gasco, P., et al. (2010) Lipid-based nanoparticles with high binding affinity for amyloid-β1−42 peptide. *Biomaterials 31*, 6519−6529.
(29) Chauhan, A., Ray, I., and Chauhan, V. P. (2000) Interaction of amyloid beta-protein with anionic phospholipids: possible involvement of Lys28 and C-terminus aliphatic amino acids. *Neurochem. Res. 25*, 423−429.
(30) Horvath, S. E., and Daum, G. (2013) Lipids of mitochondria. *Prog. Lipid Res. 52*, 590−614.
(31) Mileykovskaya, E., and Dowhan, W. (2009) Cardiolipin membrane domains in prokaryotes and eukaryotes. *Biochim. Biophys. Acta, Biomembr. 1788*, 2084−2091.
(32) Zigoneanu, I. G., Yang, Y. J., Krois, A. S., Haque, M. E., and Pielak, G. J. (2012) Interaction of α-synuclein with vesicles that mimic mitochondrial membranes. *Biochim. Biophys. Acta, Biomembr. 1818*, 512−519.
(33) Malishev, R., Shaham-Niv, S., Nandi, S., Kolusheva, S., Gazit, E., and Jelinek, R. (2017) Bacoside-A, an Indian traditional-medicine substance, inhibits β-amyloid cytotoxicity, fibrillation, and membrane interactions. *ACS Chem. Neurosci. 8*, 884−891.
(34) Malishev, R., Nandi, S., Kolusheva, S., Levi-Kalisman, Y., Klärner, F.-G., Schrader, T., Bitan, G., and Jelinek, R. (2015) Toxicity inhibitors protect lipid membranes from disruption by Aβ42. *ACS Chem. Neurosci. 6*, 1860−1869.
(35) Thapa, A., Vernon, B. C., De la Peña, K., Soliz, G., Moreno, H. A., López, G. P., and Chi, E. Y. (2013) Membrane-mediated neuroprotection by curcumin from amyloid-β-peptide-induced toxicity. *Langmuir 29*, 11713−11723.
(36) Wurth, C., Guimard, N. K., and Hecht, M. H. (2002) Mutations that reduce aggregation of the Alzheimer Aβ42 peptide: An unbiased search for the sequence determinants of Aβ amyloidogenesis. *J. Mol. Biol. 319*, 1279−1290.
(37) Oren, O., Banerjee, V., Taube, R., and Papo, N. (2018) An Aβ42 variant that inhibits intra-and extracellular amyloid aggregation and enhances cell viability. *Biochem. J. 475*, 3087−3103.
(38) Lally, C. C., Bauer, B., Selent, J., and Sommer, M. E. (2017) C-edge loops of arrestin function as a membrane anchor. *Nat. Commun. 8*, 14258.
(39) Vogel, A., Scheidt, H. A., and Huster, D. (2003) The distribution of lipid attached spin probes in bilayers: application to membrane protein topology. *Biophys. J. 85*, 1691−1701.
(40) Caspersen, C., et al. (2005) Mitochondrial Aβ: a potential focal point for neuronal metabolic dysfunction in Alzheimer's disease. *FASEB J. 19*, 2040−2041.
(41) Ly, J. D., Grubb, D. R., and Lawen, A. (2003) The mitochondrial membrane potential ($\Delta\psi$ m) in apoptosis; an update. *Apoptosis 8*, 115−128.
(42) Arispe, N., Rojas, E., and Pollard, H. B. (1993) Alzheimer disease amyloid beta protein forms calcium channels in bilayer membranes: blockade by tromethamine and aluminum. *Proc. Natl. Acad. Sci. U. S. A. 90*, 567−571.
(43) Mattson, M. P., Cheng, B., Davis, D., Bryant, K., Lieberburg, I., and Rydel, R. E. (1992) beta-Amyloid peptides destabilize calcium homeostasis and render human cortical neurons vulnerable to excitotoxicity. *J. Neurosci. 12*, 376−389.
(44) Kawahara, M., and Kuroda, Y. (2000) Molecular mechanism of neurodegeneration induced by Alzheimer's β-amyloid protein: channel formation and disruption of calcium homeostasis. *Brain Res. Bull. 53*, 389−397.
(45) Rhein, V., Baysang, G., Rao, S., Meier, F., Bonert, A., Müller-Spahn, F., and Eckert, A. (2009) Amyloid-beta leads to impaired cellular respiration, energy production and mitochondrial electron chain complex activities in human neuroblastoma cells. *Cell. Mol. Neurobiol. 29*, 1063−1071.
(46) Mutisya, E. M., Bowling, A. C., and Beal, M. F. (1994) Cortical cytochrome oxidase activity is reduced in Alzheimer's disease. *J. Neurochem. 63*, 2179−2184.
(47) Unsay, J. D., Cosentino, K., Subburaj, Y., and García-Sáez, A. J. (2013) Cardiolipin effects on membrane structure and dynamics. *Langmuir 29*, 15878−15887.
(48) Ahmed, R., Akcan, M., Khondker, A., Rheinstädter, M. C., Bozelli, J. C., Epand, R. M., Huynh, V., Wylie, R. G., Boulton, S., Huang, J., et al. (2019) Atomic resolution map of the soluble amyloid beta assembly toxic surfaces. *Chem. Sci. 10*, 6072−6082.
(49) Mannini, B., Mulvihill, E., Sgromo, C., Cascella, R., Khodarahmi, R., Ramazzotti, M., Dobson, C. M., Cecchi, C., and

https://dx.doi.org/10.1021/acschemneuro.9b00638
ACS Chem. Neurosci. 2020, 11, 1027−1037

Chiti, F. (2014) Toxicity of protein oligomers is rationalized by a function combining size and surface hydrophobicity. *ACS Chem. Biol. 9*, 2309−2317.
(50) Park, S.-Y., Kim, H.-S., Cho, E.-K., Kwon, B.-Y., Phark, S., Hwang, K.-W., and Sul, D. (2008) Curcumin protected PC12 cells against beta-amyloid-induced toxicity through the inhibition of oxidative damage and tau hyperphosphorylation. *Food Chem. Toxicol. 46*, 2881−2887.
(51) Qin, Z., Sun, Z., Huang, J., Hu, Y., Wu, Z., and Mei, B. (2008) Mutated recombinant human glucagon-like peptide-1 protects SH-SY5Y cells from apoptosis induced by amyloid-β peptide (1−42). *Neurosci. Lett. 444*, 217−221.
(52) Barrow, D. A., Lentz, B. R., et al. (1980) Large vesicle contamination in small, unilamellar vesicles. *Biochim. Biophys. Acta, Biomembr. 597*, 92−99.
(53) Panov, A. V., Lund, S., and Greenamyre, J. T. (2005) Ca 2+-induced permeability transition in human lymphoblastoid cell mitochondria from normal and Huntington's disease individuals. *Mol. Cell. Biochem. 269*, 143−152.
(54) Gnaiger, E., Kuznetsov, A. V., Schneeberger, S., Seiler, R., Brandacher, G., Steurer, W., and Margreiter, R. (2000) Mitochondria in the cold. *Life Cold 1*, 431−442.
(55) Lee, C.-p. (1979) Tightly coupled beef heart submitochondrial particles. *Methods Enzymol. 55*, 105−112.
(56) Berry, E. A., and Trumpower, B. L. (1987) Simultaneous determination of hemes a, b, and c from pyridine hemochrome spectra. *Anal. Biochem. 161*, 1−15.

https://dx.doi.org/10.1021/acschemneuro.9b00638
ACS Chem. Neurosci. 2020, 11, 1027−1037